Available online at www.scholarsresearchlibrary.com

Scholars research library

Archives of Applied Science Research, 2011, 3 (6):191-207
(http://scholarsresearchlibrary.com/archive.html)

ISSN 0975-508X
CODEN (USA) AASRC9

Biosorption of Cr(VI) and Co(II) ions from Synthetic Wastewater using Dead Biomass of Fresh Water Green Algae *Cosmarium panamense*

Onwuka J. C.[1*], Ajibola V. O.[1], Kagbu J. A.[1] and Manji A. J.[2]

[1]*Department of Chemistry, Ahmadu Bello University, Zaria, Nigeria*
[2]*Department of Chemistry, Federal University of Technology, Yola, Nigeria*

ABSTRACT

This study investigated biosorption of Cr(VI) and Co(II) ions by fresh water dead algal biomass Cosmarium panamense from aqueous solution. Batch experiments were conducted to determine the biosorption behavior of the biomass and it was observed that the adsorption capacity for Cr(VI) and Co(II) ions by the biomass are initial metal ion concentration, biosorbent dose, shaking time, pH and temperature dependent. The maximum adsorption capacities for Cr(VI) and Co(II) ions are 109.9mgCr/g and 16.69mgCo/g of the biomass respectively at initial concentration of 20ppm and pH of 2.05 for Cr(VI) and 4.05 for Co. The equilibrium data of Cr(VI) sorption was well described by Freundlich isotherm while that of Co^{2+} sorption fitted well in Langmuir isotherm model and isotherms were used to determine thermodynamic parameters of the metal ions sorption process viz free energy change, enthalpy change and entropy change and the nature of the sorption process were found to be endothermic and spontaneous in nature. Uptake kinetics of the selected heavy metals ion follow pseudo - second order model. Effect of biosorption on various properties of the algal biomass, as adsorbent, was explored in the characterization of the adsorbent were, chemical composition by EDAX , Simultaneous Thermal Analysis by TGA – DSC, Surface morphology by SEM images and surface functionality by FTIR, of the algal biomass before and after biosorption were investigated.

Keywords: Biosorption, Cd(II), Co(II), Kinetics, Thermodynamic.

INTRODUCTION

A high degree of industrialization and urbanization have substantially enhanced the degradation of aquatic environments through the discharge of industrial wastewater and domestic wastes. This has resulted in significant amount of heavy metals being deposited into natural aquatic and terrestrial ecosystems. It has also increased the biological cycling of toxic heavy metals [1]. The pollution of an aquatic environment can alter its physical, chemical and biological characteristics, jeopardizing the quality of water for human consumption [2]. Chromium, a highly reactive element with an oxidation state of 6 exhibits stability as Cr(III) and Cr(VI). But Cr(VI) is more toxic to living organisms than the Cr(III) [3]. Furthermore, Cr(III) has limited

hydroxide solubility making it relatively immobile and less available for biological uptake. Cr(VI) being powerfully carcinogenic, modifies DNA transcription process thereby causing important chromosomic aberration as quoted by The International Agency for Research on Cancer [4]. The Cr(VI) has also been classified as a group A carcinogen by USEPA based on its chronic effects [5]. Strong exposure of Cr(VI) causes cancer in the digestive tract and lungs [3] and may cause epigastric pain, nausea, vomiting, severe diarrhoea and hemorrhage [6]. Cobalt is used manufacturing glasses and ceramics and in various metallurgical processes. It enters the air and then eventually settles down to the ground and contribute to water pollution. In small amounts, cobalt is extremely beneficial to the body because it is an essential part of vitamin B12. In large amounts, cobalt becomes dangerous to the lungs and heart. Overexposure to cobalt leads to vomiting, nausea, and coma or death [7].

Conventional methods for the removal of heavy metals from wastewaters, however, are often cost prohibitive having inadequate efficiencies at low metal concentrations, particularly in the range of 1–100 mg/l. Some of these methods, furthermore, generate toxic sludge, the disposal of which is a burden on the techno-economic feasibility of treatment procedures. These constraints have caused the search for alternative technologies for metal sequestering to cost-effective environmentally acceptable levels. The ability of biological materials to adsorb metal ions has received considerable attention for the development of an efficient, clean and cheap technology for wastewater treatment at metal concentrations as low as 1 mg/l. Several materials in the categories of microbial biomass such as yeast, bacteria, fungi, algae and plant wastes have been successfully used for metal biosorption [8]. Among the biological materials marine alga have been reported to have high metal binding capacities due to the presence of polysaccharides, proteins or lipid on the cell wall structure containing functional groups such as amino, carboxyl, hydroxyl and sulphate, which can act as binding sites for metals [9].

The aim of this work was to study the biosorption of Cr(VI) and Co(II) ions from aqueous solutions using dead biomass of fresh water green algae *Cosmarium panamense*. The influence of contact time, initial metal ion concentration, temperature, biosorbent dose and initial solution pH on biosorption of Cr(VI) and Co(II) was studied. The biosorbent was characterized by employing instrumental techniques, viz., Fourier transform infrared spectroscopy (FTIR), Simultaneous thermal analysis (STA) and scanning electron microscope (SEM). The equilibrium and kinetics were obtained from batch experiments. Both the Langmuir and Freundlich isotherm models were evaluated to examine biosorption capacity of *Cosmarium panamense* for Cr(VI) and Co(II) ions.

MATERIALS AND METHODS

2.1 Chemicals

Analytical Reagent Grade Chemicals and Distilled De-ionized water were used. They are: Conc. $HNO_{3(aq)}$, $NaOH_{(s)}$, $NaNO_{3(s)}$, $k_2Cr_2O_{7(s)}$, and $Co(NO_3).6H_2O_{(s)}$. Cr(VI) and Co(II) solutions of different concentrations were obtained by diluting their respective stock solutions (1000mg/l) which was prepared using 0.01M $NaN0_3$. Standard acids and base solutions (0.1M HCl and 0.1M NaOH) were used for pH adjustments.

2.2 Equipments

Carbolite Furnace Model (GLM-3), Continent Microwave Oven (MW800G), Analytical Digital Balance (GR-200-EC), Top Loading Balance – XP500, Endecotts Sieve with Mechanized Shaker, Thermostat Water Bath Shaker, pH Meter (CRISON MICRO pH 2000), Atomic Absorption Spectrophotmeter, Shimatzu Fourier Transform Infra-red, Hitachi s – 540 with

Oxford Instruments 7497 EDAX, Using link ISIS Computer Software, SDT Q600 V4.1 Build 59.

2.3 Biosorbent preparation

Fresh algal biomass was collected from swimming pool located at Ahmadu Bello University, Zaria, Nigeria. Before use, it was washed several times with tap water and then with de-ionized water to remove impurities and salts. The biomass was sun –dried and then dried in an oven at 60^{o}C for 48hours. The dried algae biomass was cut, grinded in a mortar and subsequently sieved and particles with an average size 0.5mm was used for biosorption experiments.

2.4 Batch adsorption studies

The experiment was carried out at ambient temperature (25^{o}C) in a shaker water bath using 100ml conical flask as the reactor.

All the solutions was prepared in 0.01M $NaNO_3$ solution using de-ionized water. The $NaNO_3$ serve as background inert electrolyte that provides stability in the ionic strength of the solution throughout the experiment. The pH of the solution was adjusted to the required value throughout the experiment with 0.1M NaOH and 0.1M HNO_3. This gave only nitrate ion and sodium ion which are already in the medium without altering the chemistry of the ion of interest.

The experiment was carried out as follows:
50ml of each of the working solution was measured using standard flask into three 100ml conical flask. This makes a triplicate for a given concentration i.e a set. 0.1g of the adsorbent was transferred into each of these conical flasks; the pH of the mixture was measured and adjusted to the desired pH. Chromium – 2.05, and Co pH – 4.05. Each set was agitated in the shaker at the same time for 3hrs and the set was left undisturbed on the desk for 24hrs to allow the system to equilibrate. After 24hrs the mixture was filtered through a whatman filter paper into 120ml polyethylene bottle. The first 5mls of the filtrate was discarded. This allows the filter paper to saturate with the solution. The concentration of the residual metal ion remaining in the solution was determined using AAS.

The amount of the metal adsorbed was calculated using the equation below

$$q_e = \frac{\mathrm{V\,(C_o - C_e)}}{\mathrm{M}}$$

Where q_e is the amount of adsorbate ion adsorbed in milligram per gram of the adsorbent, C_o is the initial concentration of the metal ion before adsorption process, C_e is the equilibrium concentration of the metal ion in the filtrate after adsorption process and M is the mass in gram of the adsorbent, V is the volume of the solution.

RESULTS AND DISCUSSION

3.1 Characterization of the Biosorbent

Scanning electron microscope clearly revealed the surface texture and morphology of the algal biomass before and after biosorption at 500x magnification (Fig.1). Uneven surface texture along with a lot irregular surface format was observed. SEM photos displayed evidently that over the biosorption period, the surface morphology of the native algal biomass had undergone remarkable physical disintegration resulting to emergence of protrusions and rough surface area. Similar SEM observations were reported by other researchers [10-13].

Table 1.Summary of Elemental Analysis using EDAX

Native Biomass	Cr(VI) Treated Biomass	Co(II) Treated Biomass
Carbon	Carbon	Carbon
Oxygen	Oxygen	Oxygen
Aluminium	Aluminium	Aluminium
Niobium	Niobium	Niobium
Chlorine	Chlorine	Chlorine
Copper	Copper	Copper
----------	Silicon	Silicon
----------	----------	Iron
	Chromium	Cobalt

Energy dispersive x – ray is used to detect elements amounts that are up to 0.1%. High presence of carbon, oxygen, aluminum, copper, silicon, iron, niobium and chlorine in the algal biomass was observed from visual analysis of Fig.2. It was also observed that the number of elements detected by the energy dispersive x – ray on the biomass before and after biosorption varies (Table 1). This is due to the surface interactions of each of this heavy metal (Cr(VI) and Co^{2+}) ions on the surface binding sites of the algal biomass during biosorption resulting to complexation and ion – exchange which affects the availability of these elements for detection. This goes in line with the reports in literature by Ahalya *et al.*,[14] that Non – metabolism dependent biosorption mechanism is a rapid process that include precipitation, physical adsorption, ion – exchange, and complexation.

Thermal stability of the algal biomass *Cosmarium panamense* before and after biosorption was evaluated by simultaneous thermal analysis. This was performed by TGA – DSC curves with a heating rate of 50^{o}C/min under nitrogen atmosphere within the temperature range of 50 – 600^{o}C and DSC scanning range of 0 – 120mcal/sec (Fig.3). The biomass samples showed two step decomposition process but the percentage weight residue after was lower after biosorption, which suggest that biosorption affects the inorganic content of the biomass. Also the heat required for thermal degradation was higher after biosorption, which is as a result of the ionic bond formed after biosorption. The stability showed by the biomass suggests that the biomass is responsible for the biosorption of these metal ions. This was similarly reported by Venkatamohan *et al.*, [15] and Gupta and Rastogi [10].

The FTIR spectra of native and different heavy metal ions (Cr(VI) and Co^{2+}) treated algal biomass in the range of 500 – 5000cm^{-1} were performed to have an idea of which functional groups were responsible for the biosorption process (Fig.4). It was observed from that the absorbance peaks of the different heavy metal ions treated algal biomass were slightly lower than the absorbance peaks of native algal biomass. Band shift that appeared at 534.3cm^{-1} represents the C – N – S scissoring which are found in polypeptide structure [10] and Si – O – Si bend of the silica group [16]. This further supports the earlier detection of silicon by EDAX in the algal biomass samples. The absorption band observed at 1030.99cm^{-1} could be assigned to C – N, C – OH and P – O – C stretching vibrations of amines and Proteins fractions [17][18][19]; polysaccharides [20] and phosphonate groups respectively [21][22]. The peak appearing at 1435.09cm^{-1} could be attributed to C – H bending of methyl and methylene functional group [23][20]. The absorption band at 1654.01cm^{-1} may be as a result of –C = C (characteristics of alkene), - C = N, - C = O stretching and N – H bending of amines or amide I and amide II band of amide bond of protein peptide bonds [10, 18-24]. The peak observed at 2927.08cm^{-1} could be assigned C – H stretching of methyl and methylene group in cell wall structure [17,18,12] and asymmetric stretching of carboxylate anion (- COO^{-}) [21][10]. The display of strong broad – OH

(H bonded) and – NH stretch of carboxylic and amine band respectively were also observed in the region of 3453.66cm^{-1} [18]. The spectra analysis indicate the presence of ionizable functional groups namely amino, amide, carboxyl, phosphonate, hydroxyl, silica, methyl and methylene group which are able to interact with proton or metal ions. The FTIR spectra result obtained is consistent with published FTIR spectra reports by other researchers [10, 18-24].

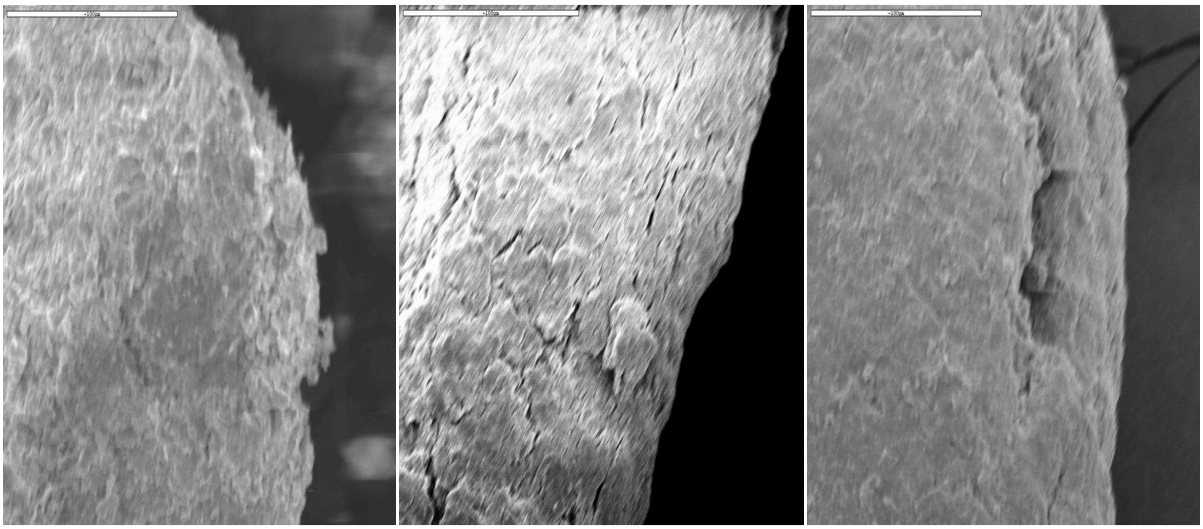

(a) (b) (c)

Fig.1 SEM micrograph at 500x magnification of the different algal biomass (a) Native (b) Cr(VI) treated (c) Co^{2+} treated algal biomass.

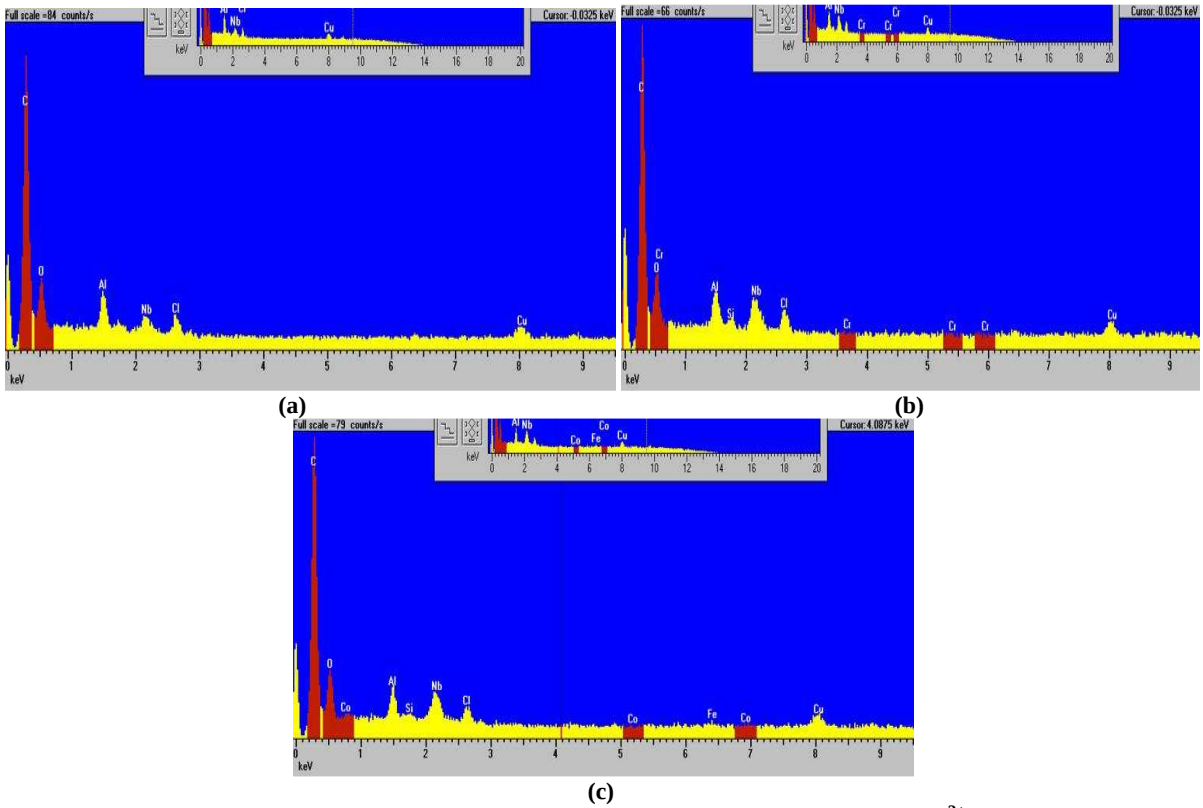

(a) (b)

(c)

Fig.2 EDAX Profile of the different algal biomass (a) Native (b) Cr(VI) treated (c) Co^{2+} treated algal biomass.

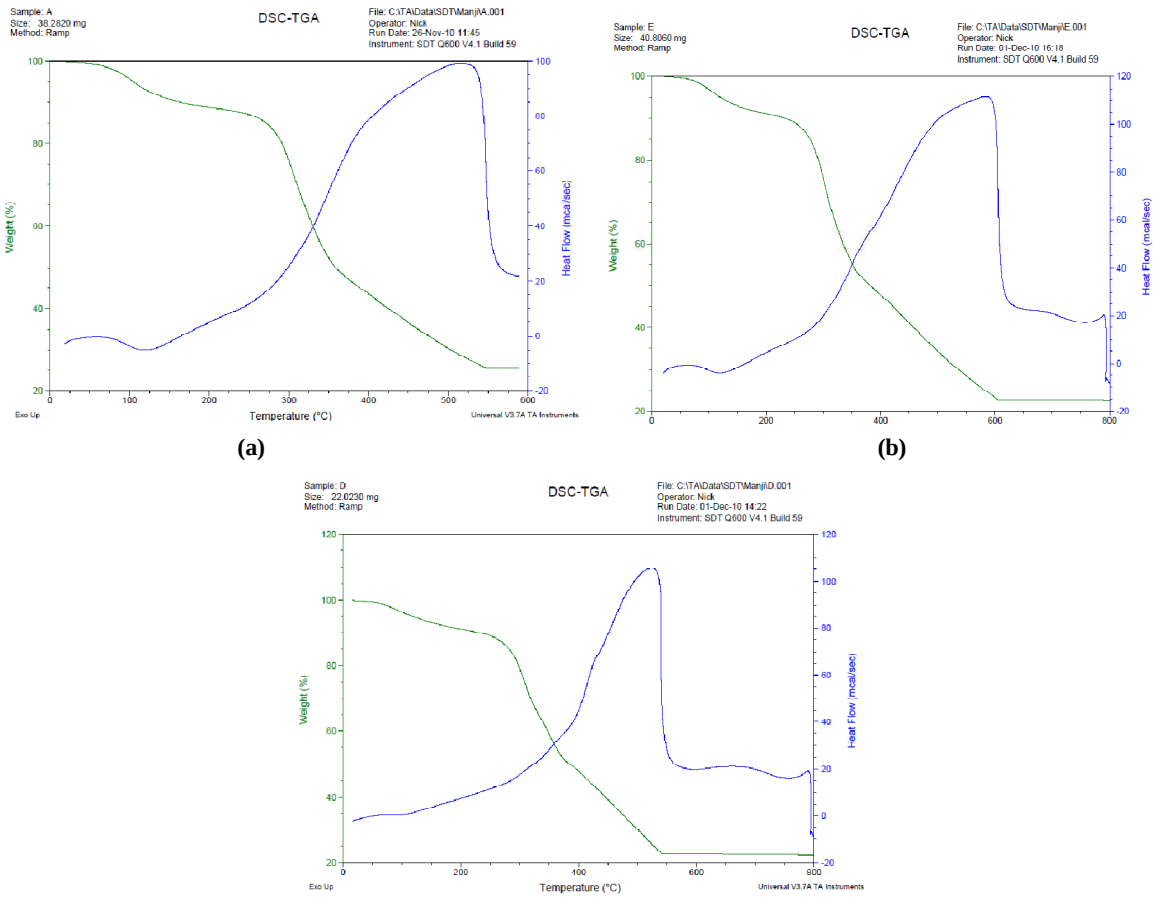

Fig.3 Thermogram of the algal biomass (a) Native (b) Cr(VI) treated (c) Co^{2+} treated algal biomass

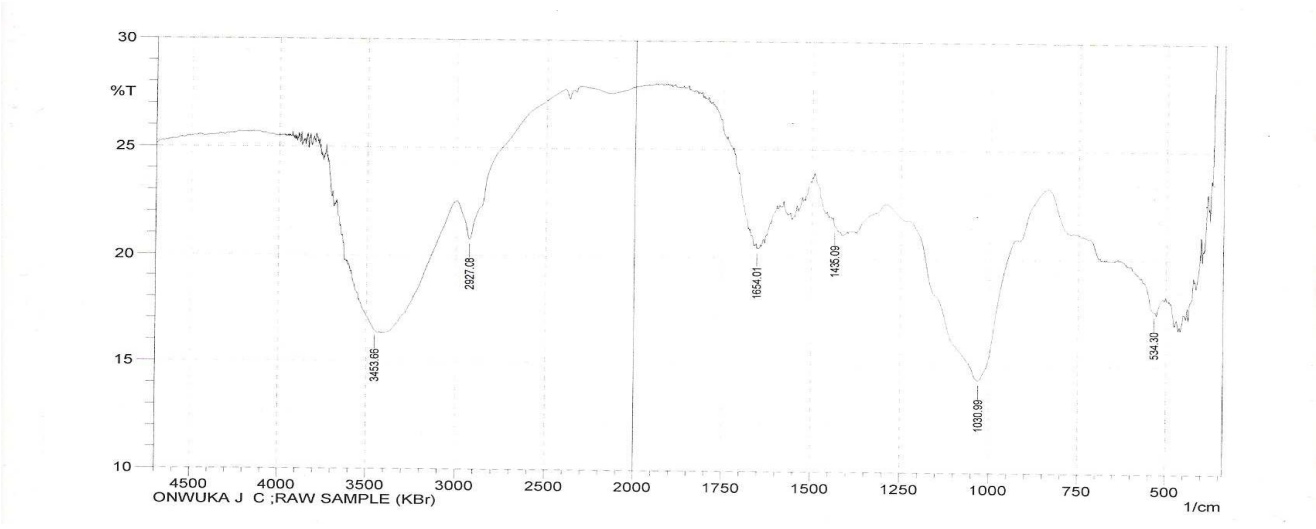

(a)

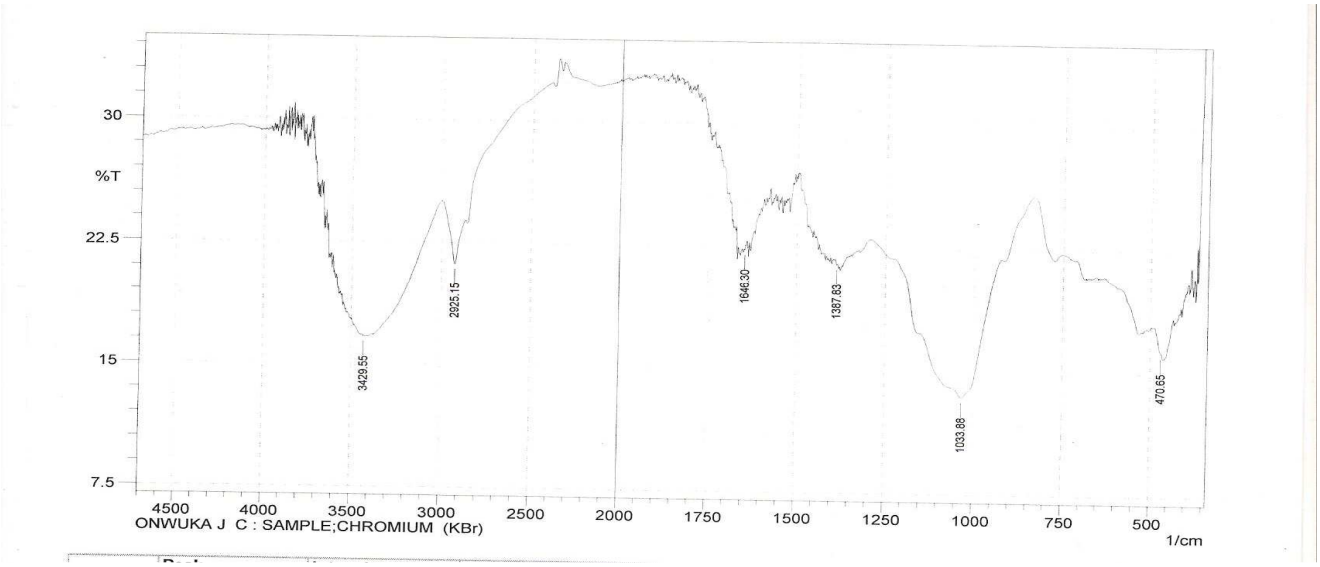

(b)

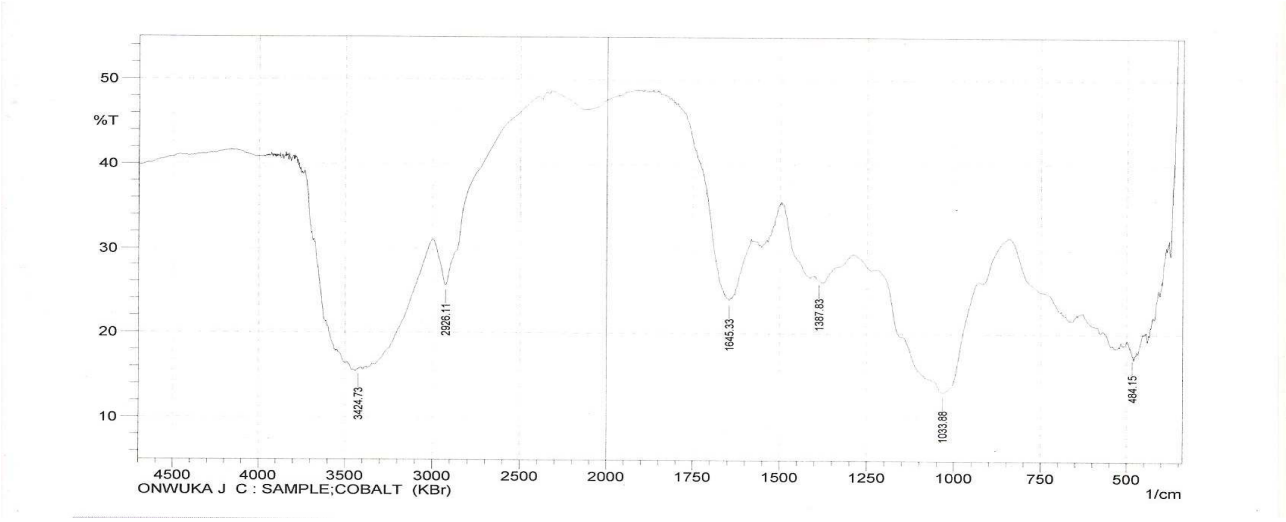

(c)

Fig.4. FTIR Spectra of algal biomass (a) Native (b) Cr(VI) treated (c) Co^{2+} treated algal biomass

3.2 Biosorption of heavy metal ions

3.2.1 Effect of initial metal ion concentration

This was studied at constant biomass concentration, pH, and temperature were by varying the initial metal ion concentration (5, 10, 15, 20, and 25ppm) of each of the metal ion. The metals showed highest metal uptake at initial metal concentration of 25ppm. It was observed that as the initial metal ion concentration of the various metals was increased, the respective metal uptake also increased (Fig.5). It has been reported that with increasing metal ion concentration, the specific sites are saturated and vacant sites are filled and at low concentrations adsorption sites took up the available metal more rapidly or quickly while at higher concentrations metal ions need to diffuse to the biomass surface by intra particle diffusion and greatly hydrolyzed ions will diffuse at a slower rate [25][26][27].

3.2.1.1 Biosorption modeling

To estimate the sorption capacity of the algal biomass, the isotherm data were analyzed using adsorption type isotherm models. The Langmuir and Freundlich isotherms are the most commonly used for solid – liquid phase isotherms. These isotherms relate the amount of metal

ion sorbed at equilibrium per unit weight of the sorbent, q_e(mg/g) to the sorbate concentration at equilibrium, C_e(mg/l). The linearized form of Langmuir isotherm can be expressed as:

$$\frac{1}{q_e} = \frac{1}{q_{max}} + \frac{1}{bq_{max}C_e} \quad \text{.....(1)}$$

Where; q_e is the amount of adsorbate adsorbed per gram of dried adsorbent at equilibrium (mg adsorbate/g of dried adsorbent), q_{max} is the constant relating to the maximum amount of adsorbate ion bound per g of adsorbent for a monolayer (mg/g), b is Langmuir constant or adsorption coefficient or the adsorption affinity (l/mg) for binding of adsorbate on the adsorbent sites and C_e is equilibrium (residual) adsorbate concentration in solution after sorption (mg/l).

The values of q_{max} and b can be calculated from the intercept $\left(\frac{1}{q_{max}}\right)$ and slope $\left(\frac{1}{q_{max}b}\right)$ of the plot $\frac{1}{q_e}$ against $\frac{1}{C_e}$ as illustrated in Figures 6(a) and 7(a).

The Freundlich isotherm model describe non – ideal sorption onto heterogeneous surfaces involving multilayer sorption. The isotherm model linearized form is given as

$$lnq_e = lnK_F + \frac{1}{n} ln\, C_e \quad \text{..... (2)}$$

Where, q_e is the amount of adsorbate adsorbed per unit weight of biosorbent, K_F is Freundlich Constant measuring adsorption capacity(L/mg), C_e is equilibrium concentration of the adsorbent in solution(mg/l), n is constant related to adsorption efficiency and energy of adsorption or adsorption intensity of the adsorbent.

Figures 6(b) and 7(b) shows Freundlich isotherm model the different heavy metal ions biosorption and the isotherm constants and correlation coefficients, R^2, are also listed in Table 2. A plot of lnq_e against lnC_e gives a straight line with a slope, 1/n and an intercept of lnK_F. The K_F value increases with the total adsorption capacity of the adsorbent to bind the adsorbate. The numerical value of n is a useful index to determine favorability of the adsorption.

Table 2: Langmuir and Freundlich isotherm constants for the biosorption of the Selected Metal ions on algal biomass (*Cosmarium panamense*)

Metals	Langmuir Constant				Freundlich Constant		
	q_{max}(mg/g)	b(Lmg^{-1})	b(Lmol^{-1})	R^2	$1/n$	K_f(mg/g)	R^2
Chromium	109.9	0.15	7800	0.9969	0.97	14.50	0.9991
Cobalt	16.69	0.05	2950	0.9919	0.75	1.01	0.9572

Table 2 showed that the equilibrium data for Cr(VI) sorption fitted reasonably well to the linearized equation of the Langmuir isotherm over the whole concentration range studied. From linear correlation coefficients of the adsorption isotherm, it is noted that the Freundlich isotherm model exhibits better fit to the sorption data of Cr(VI) than the Langmuir isotherm model. This phenomenon suggests that multilayer sorption takes place on the surface of the algal biomass during Cr(VI) ion sorption [28].

It was also observed that data for Co^{2+} sorption are not well fitted to Freundlich model of sorption. In other words, the equilibrium data was well represented by Langmuir isotherm equation when compared to Freundlich isotherm because Langmuir isotherm possess higher

correlation coefficient than Freundlich isotherm correlation coefficient for Co^{2+} sorption. The high degree of correlation for the linearized Langmuir relationship suggest monolayer sorption on specific sites or single surface reaction for Co(II) ion [10].

The values of in Table 2 falls within 0 – 1 range which strongly suggest favorable adsorption. The values of n, which is related to the distribution of bonded ions on the sorbent surface, represent beneficial adsorption if is between 1 and 10. The n values for the biosorbent used, was found to be greater than one, indicating that adsorption of Cr (VI) and Co(II) is favorable [28].

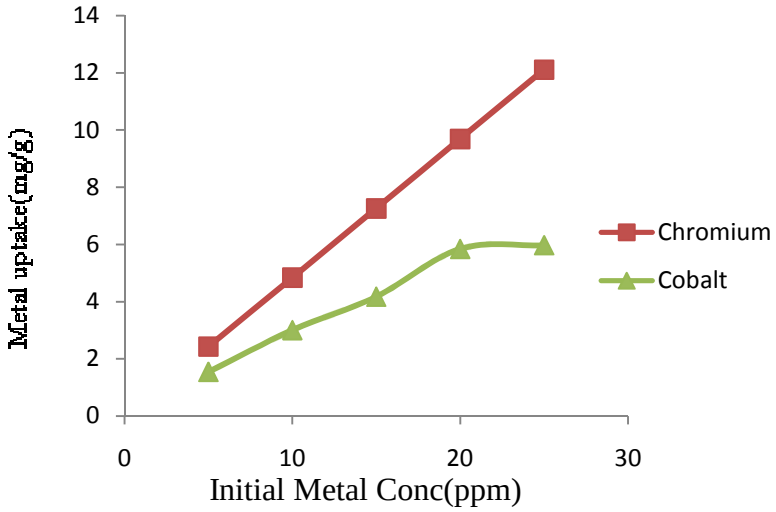

Fig.5: Effect of initial metal ion concentration

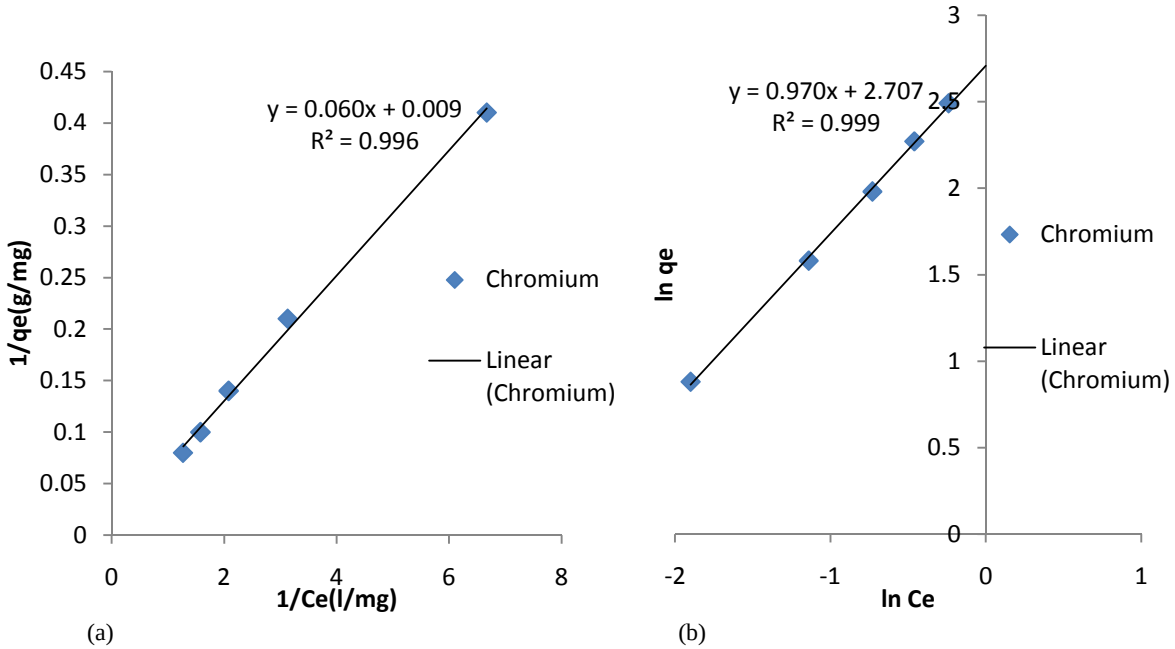

(a) (b)

Fig.6: Isotherm modeling for Cr(VI) biosorption (a) Langmuir (b) Freundlich biosorption isotherm for Cr(VI) biosorption

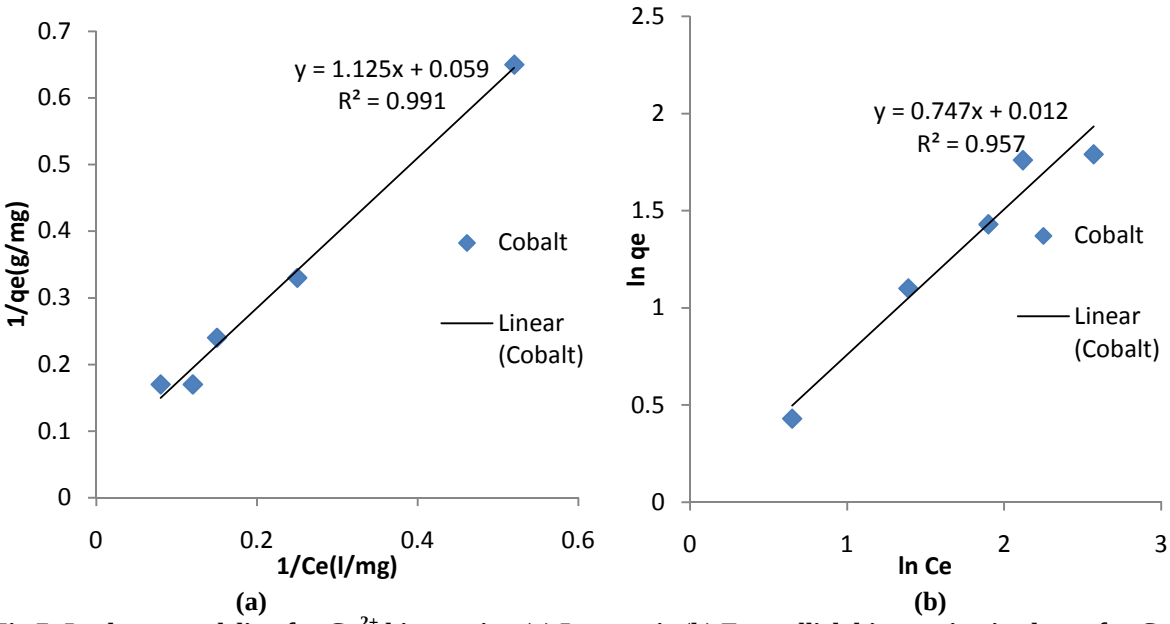

Fig.7: Isotherm modeling for Co^{2+} biosorption (a) Langmuir (b) Freundlich biosorption isotherm for Co^{2+} biosorption

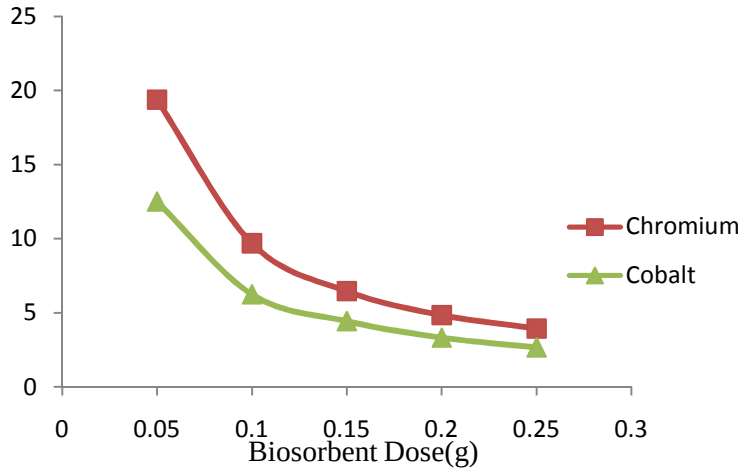

Fig.8: Effect of biosorbent dose

3.2.2 Effect of Biosorbent Dose

Figure 8 revealed that the heavy metal ions showed a unique biosorption behavior at the various biosorbent dosage. As the biosorbent dose increases, the removal efficiency increases while the metal uptake decreases. Therefore, 0.05g of the adsorbent comparatively showed the lowest removal efficiency and highest adsorption capacity while 0.25g of the adsorbent gave the highest removal efficiency and lowest adsorption capacity for all the metals. It has been reported by Pattabhi *et al.*, [29] that increase in biomass concentration increases the level of biosorption due to the overall increase in surface area of the biomass which in turn increases the number of binding sites. Saradhi *et al.*, [27] explained that the metal uptake (mg/g) decreases with increase in biosorbent dose due to the interference of inter – particle cohesive forces, interference of binding sites, desorption due to abrasion, turbulence and reduce mixing due to large mass of the biosorbent while Rastogi and Gupta, [10] attributed this to the fact that at higher adsorbent dose, the availability of higher energy sites decreases with a larger fraction of lower energy sites occupied. It has been suggested that electrostatic interaction between cells can be a significant factor in the relationship between biomass concentration and metal sorption, in this connection,

at a given metal ion concentration, the lower the biomass in suspension, the higher will be metal/biomass ratio and the metal retained by sorbent unit unless the biomass reaches saturation. High biomass concentration can exert a shell effect protecting the active sites from being occupied by metal and this results to lower specific metal uptake [30].

3.2.3 Effect of contact time

The contact time was evaluated as one of the important parameters affecting the biosorption efficiency. Fig.9 showed that the maximum adsorption for Cr(VI) and Co^{2+} (9.84mg/g and 6.67mg/g respectively) occurred at 90min and 120min respectively. It was also observed that process of adsorption was high at the initial stage and became slower while approaching the equilibrium stage. This is obvious due to the fact that more number of vacant negatively charged sites are available initially on the surface of the adsorbent and the sites are gradually filled up while approaching equilibrium and completely filled at equilibrium [27]. Contact time were further used to generate the rate of the reaction.

3.2.3.1 Biosorption kinetics

In order to investigate the mechanism of biosorption and potential rate controlling step, pseudo first order and pseudo second order kinetic models were used to test the equilibrium data
The pseudo first-order equation [31] is generally expressed as [32]:

$$\log(q_e - q_t) = \log q_e - \frac{k_1 t}{2.303} \quad \text{.....(3)}$$

Where q_e and q_t are the amount of sorbate adsorbed on adsorbent at equilibrium and time *t*, respectively (mg/g), and k_1 is the rate constant of first order adsorption (min^{-1}).

The plot of $\log(q_e - q_t)$ versus t will give a straight line and the value of k_1 can be evaluated from the slope of the graph, $-\frac{k_1}{2.303}$, while $q_{e(\text{calculated})}$ is obtained from the intercept, log q_e, of the graph as illustrated in Fig.10(a) and 11(a).

The linearized second-order kinetic model is expressed as [33]:

$$\frac{t}{q_t} = \frac{1}{k_2 q_e^2} + \frac{1}{q_e} t \quad \text{.....(4)}$$

Where, k_2 is the pseudo-second-order rate constant of adsorption (g $mg^{-1}min^{-1}$). The plot of $\frac{t}{q_t}$ versus t will give a linear relationship with $\frac{1}{q_e}$ and $\frac{1}{k_2 q_e^2}$ as a slope and intercept, respectively. The values of q_e and k_2 can be determined from the slope and intercept as illustrated in Fig.10(b) and 11(b).

Table 3: Comparison between adsorption rate constants, q_e estimated and correlation coefficient associated to the Lagergren pseudo first – and second – order adsorption.

	Pseudo First – Order Model			$q_{e\,\text{exp.}}$	Pseudo Second – Order Model		
	$q_{e(\text{cal})}$	$K_1(min^{-1})$	R^2	(mg/g)	$q_{e(\text{cal})}$	$K_2(gmg^{-1}min^{-1})$	R^2
Chromium	0.120	- 0.016	0.6726	9.84	9.95	0.088	0.9999
Cobalt	0.480	-0.002	0.1893	6.67	6.96	0.021	0.9983

It was found that the correlation coefficients for pseudo second order model is higher than that of pseudo first order (Table 3). Hence, the correlation coefficients and calculated adsorption capacities of the metal ions sorption by pseudo first order model are not satisfactory, which suggest that they are dependent on initial concentration. However, Pseudo second order adsorption model is more suitable to describe the adsorption kinetics of Cr(VI) and, Co^{2+} on algal biomass and this relies on the assumption that biosorption may be the rate-limiting step [10]. The obtained kinetic information has a significant practical value for technological applications, since kinetic modeling successfully replaces time and material consuming experiments, necessary for process equipment design [26]. This is supported by other reports [10][34][20][18].

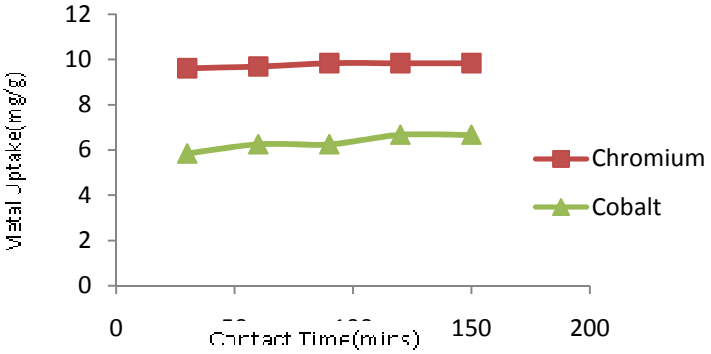

Fig.9: Effect of contact time

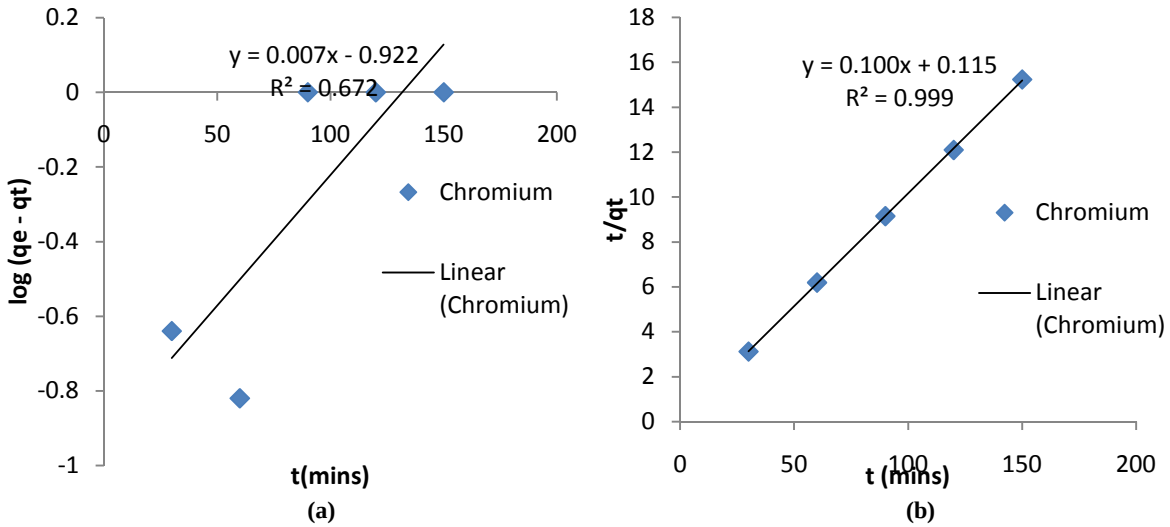

Fig.10: Kinetic modeling for Cr(VI) biosorption (a) pseudo first order (b) pseudo second order kinetic modeling

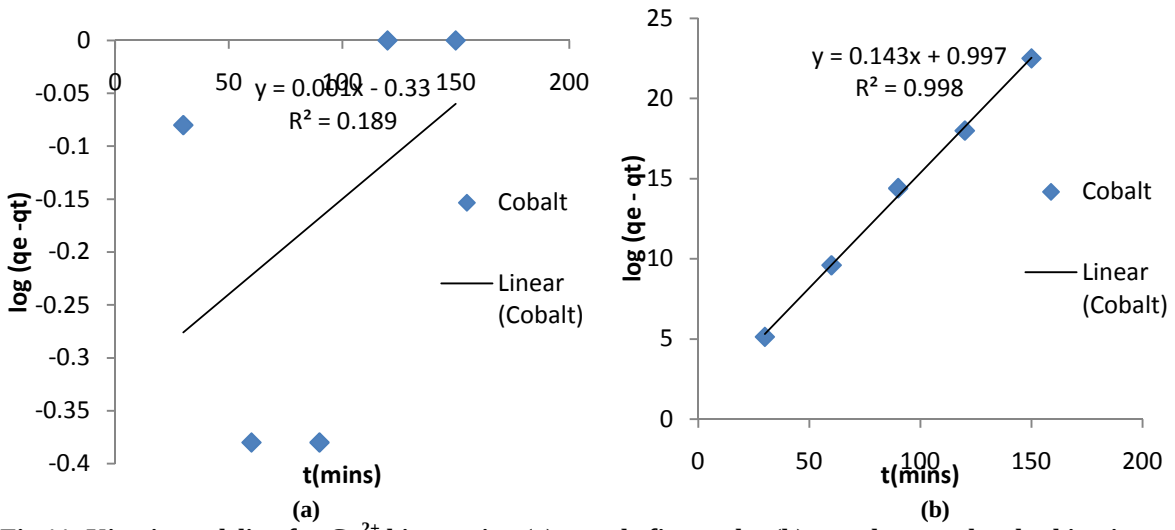

Fig.11: Kinetic modeling for Co^{2+} biosorption (a) pseudo first order (b) pseudo second order kinetic modeling

3.3.3 Effect of initial solution pH

The pH of the solution influence both metal binding sites on the cell surface and the chemistry of metal in solution [35]. It was observed that both the adsorption capacity and removal efficiency of Cr(VI) decreases as the pH of the solution increases (Fig.12). The increased binding of hexavalent chromium at low pH can be explained by two factors. First, adsorption of Cr(VI) at pH 2.0 suggests that the negatively charged chromium species (chromate/dichromate in the medium) bind through electrostatic attraction to positively charged functional groups on the surface of biosorbents. As the pH increased, the overall surface charge on the cells became negative and biosorption decreased. In alkali conditions, carboxylate group exists in deprotonated form and has net negative charge. As a result, the surface charge of the biosorbents become negative and biosorption of Cr(VI) decreases. Secondly, the solution chemistry of Cr(VI) ions can affect the biosorption process. Previous studies showed that chromium exhibits different types of pH dependent equilibria in solutions. Sorbate and chromium form stable complexes such as $Cr_2O_7^{2-}$, $HCrO_4^-$, CrO_4^{2-}, and $HCr_2O_7^-$, the fraction of any particular species is dependent on chromium concentration and pH. In low chromium concentration, the main fraction is $HCrO_4^-$ with pH below 5.0, whereas the CrO_4^{2-} increases with increase of pH value and becomes the main form with pH above 7.0 [12][17][36].

Fig.12 also showed that as the solution pH of Co^{2+} was increased, its adsorption capacity first increased from 2 pH to pH 6 and then decreased at pH 8. This may be attributed to the same reason as in Cr(VI), at pH higher than 6, formation of insoluble metal hydroxides or anionic hydroxide complexes of metal ions takes place restricting the true biosorption studies. This is consistent with the results obtained for the other adsorbent systems [18, 29-31, 34, 37].

3.3.4 Effect of Temperature

It was observed that the metals showed increase in adsorption capacity with increase in temperature (Fig.13). This could be due to increase in average kinetic energy of the metal ions in solutions containing the adsorbent which increases the number of metal ions interacting with the adsorbent surface by increasing the rate at which the metal ions hit the binding sites at the surface of the adsorbent thus increasing the adsorption capacities. The equilibrium data obtained was further used for thermodynamic modeling to determine the enthalpy, entropy and free energy of the adsorption reaction at different temperatures.

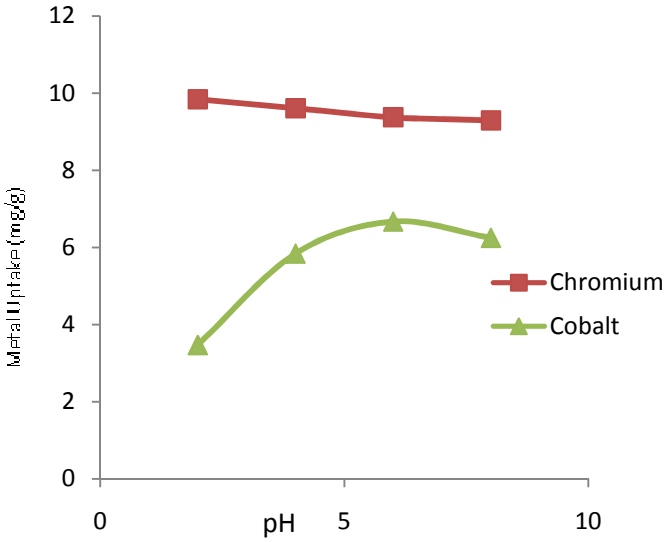

Fig.12: Effect of initial solution pH

3.3.4.1 Thermodynamic modeling

Thermodynamic parameters were obtained by varying the temperature conditions while other variables constant were kept constant [28]. The thermodynamic parameters such as change in standard free change energy (ΔG^o), enthalpy change (ΔH^o) and entropy change (ΔS^o) for adsorption process are calculated from binding energy constant, *b*, obtained from Langmuir equation using the following thermodynamic equations:

$$\Delta G^\circ = -RT\ ln(b) \quad \text{.....(5)}$$

$$\Delta G^\circ_{ads} = \Delta H^\circ_{ads} - T\Delta S^\circ_{ads} \quad \text{.....(6)}$$

Where: R (8.314
J/mol K) is the gas constant, T (K) the absolute temperature and *b* (L/mol) is the Langmuir constant related to free energy or net enthalpy of adsorption. By plotting a graph of
versus *T*, the values ΔH^o and ΔS^o can be estimated from the intercept and slope

Table 4: Calculated values of Gibbs Free Energy in Jmol^{-1} of the metals sorption process over the temperature range studied

Temp.(K)	Chromium	Cobalt
300	-22352.7	-19927.5
313	-23321.3	-20791.1
323	-24066.4	-21455.3
333	-24811.5	-22119.5

Table 5:Thermodynamic parameters for the biosorption of the metals on the algal biomass.

	Chromium	Cobalt
(Jmol^{-1})	0.0474	0.4912
(Jmol^{-1} K^{-1})	74.509	66.427

Free energy change of the metal ions adsorption process was found to be negative (Table 4), suggesting spontaneous process. In general, it is of note that free energy up to −20 kJ/mol are consistent with electrostatic interaction between charged molecules and surface indicative of

physiosorption while more negative than −40 kJ/mol involve chemisorption, free energy change values between −20 to −40 kJ/mol indicate that both physisorption and chemisorption were responsible for adsorption [26]. Thus, the magnitude of the free energy change values obtained in this study indicates both physical and chemical mechanism for the adsorption of Cr(VI) and Co(II) ions on to the *Cosmarium panamense* algal biomass, hence physiosorption and chemisorption were responsible for their adsorption.

The values of enthalpy change for the sorption of the metal ions were positive(Table 5), which suggest endothermic reaction and could be attributed to increase in adsorption on successive increase in temperature while the positive values of entropy reveals increase in randomness at the solid – solution interface during the fixation of the different metal ions on the active sites of the biosorbent [10]. This could be as a result of high affinity for these metal ions by the binding sites on the surface of the algal biomass. Gupta and Rastogi, [10] reported that if adsorption process is endothermic, it means under the conditions the process becomes spontaneous because of the large positive entropy change.

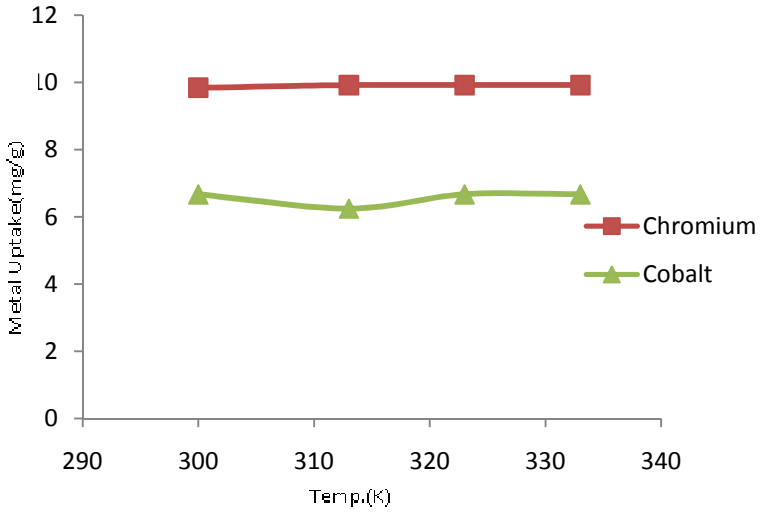

Fig.13: Effect of temperature

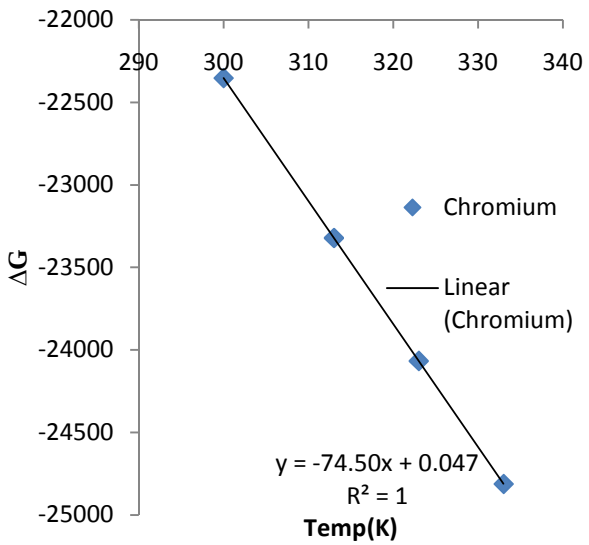

Fig.14: Thermodynamic modeling for Cr(VI) biosorption.

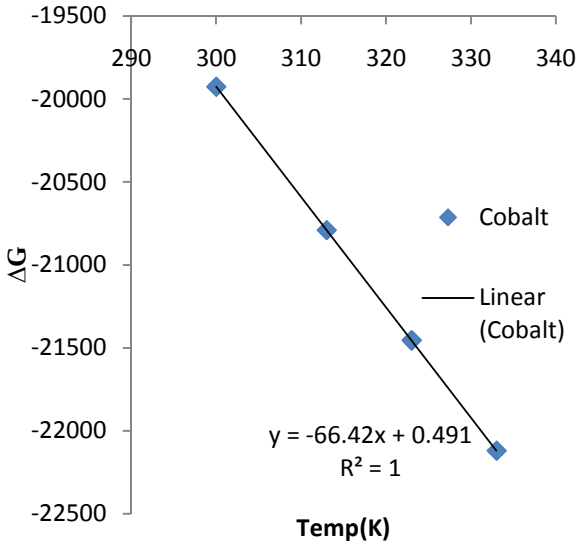

Fig.15: Thermodynamic modeling for Co^{2+} biosorption

CONCLUSION

• The batch studies conducted proves that biosorption of Cr(VI), and Co(II) ions on dead biomass of green algae *Cosmarium panamense* species are dependent of initial solution pH, initial metal ion Concentration, biosorbent dosage, contact time, and temperature.
• It was found that the adsorption data for Cr(VI) ion sorption was better fitted to Freundlich adsorption model while the adsorption data Co^{2+} sorption fitted well to Langmuir adsorption model. Hence, biosorption of Cr(VI) ion on the algae biomass is a multilayer sorption process while that of Co^{2+} is a monolayer sorption process.
• Thermodynamic modeling showed that physiosorption and chemisorption process were involved in the biosorption of these metals and these processes are spontaneous and endothermic.
• The availability of elements in the algal biomass, for detection are affected by biosorption of these metals on algal biomass. Hence, the inorganic status of the algal biomass are influenced by biosorption.
• Simultaneous thermal analysis reveals that both the native and the different heavy metal treated algal biomass are thermally stable but with different energy and inorganic composition status.
• FTIR showed that carboxyl, hydroxyl, amines, amides, alkenes, alkynes, phosphonate and silica functional groups functional groups are responsible for the adsorption of these selected heavy metals.

Acknowledgement
Authors are thankful to Department of Chemistry, Ahmadu Bello University (ABU), Zaria; Department of Chemistry, Bangor University, North Wales, United Kingdom; and National Research Institute for Chemical Technology (NARICT), Zaria.

REFERENCES

[1] Nilanjana Das, Karthika, P, Vimala R, and Vinodhini V.(**2008**). *Natural Product Radiance*, Vol.7(2), Pp 133 – 138.
[2] Marques, P.A.S.S., Rosa, M.F., Mendes, F., Pereira, M.C., Blanco, J. and Malato, S., (**1996**). *Desalination*, 108, 213-220.
[3] Kaufaman, D. B.(**1970**). *American journal of disease of children*, 119, 374–381.
[4] Cieslak-Golonka, M.(**1995**). *Polyhedron*, 15, 3667–3689.
[5] Nkhalambayausi-Chirwa, E. M., and Wang, Y. T.(**2001**). *Water Research*, 35, 19221–21932.
[6] Browning, E.(**1969**). Chromium in Toxicity of Industrial Metals, second ed., Butterworths and Co, London, 1969, pp. 76–96.
[7] Mayflor Markusic (**2009**). Effects of potentially Toxic Metals. Niki fears publishers, florida.
[8] Sumathi, K. M. S., Mahimairaja, S., and Naidu, R.(**2004**). Use of low-cost biological wastes and vermiculite for removal of chromium from tannery effluent. Bioresource Technology.
[9] Davis T.A., Volesky B., and Mucci A.,(**2003**). *Water. Res.* 37, 4311-4330.
[10] Gupta, V. K, and Rastogi, A (**2007**). *J.Colloid Interface Sci.*
[11] Shakirullah, M., Habib-ur-Rehman, Imtiaz Ahmad, Sher Shah and Hameedullah(**2006**). *Journal of the Chinese Chemical Society*, 53: 1045-1052.
[12] Sethuraman, P and Balasubramanian, N.(**2010**). *International Journal of Engineering Science and Technology.* Vol. 2(6): 1811-1825.
[13] Wilke, A., Buchholz, R., and Bunke, G.,(**2006**), *Environ. Biotechnol*. 2: 47 – 56.
[14] Ahalya N, Ramachandra T. V, and Kanamadi R. D (**2003**). Biosorption of Heavy Metals. *Research Journal of Chemistry and Environment*. Vol.7 (4).

[15] Venkatamohan, S., Ramanaiah, S. V., Rajkumar, B., and Sharma, P. N.(**2007**). *J. Hazard. Mater*. 141: 465–474.
[16] 16. Nwankwere, E. T. O. (**2010**): Acetylation of Rice (*Oriza Sativa*) Husk for Oil Spillage Treatment Using N – Bromo Succinimide As Catalyst. Unpublished M.Sc. Thesis, Department of Chemistry, Ahmadu Bello University, Zaria.
[17] Park, D., Yeoung – Sang, Y., and Jong, M. P.(**2005**). *Chemosphere* 60: 1356 – 1364.
[18] Ansari, T. M., Umbreen, K., Nadeem, R., and Hanif, M. A.(**2009**). *African Journal of Biotechnology* Vol. 8 (6), pp. 1136-1142.
[19] Gochev, V. K., Velkova, Z. I and Stoytcheva, M. S.(**2010**). *J. Serb. Chem. Soc*. 75 (4): 551–564.
[20] Krishnaiah, A., Kalyani., Sankara Reddy V. S. G., Boddu, V. M. and Subbaiah, M. V. (**2008**). *E-Journal of Chemistry*, Vol. 5, No.3, pp. 499-510.
[21] Choi, S. B., and Yun, Y. S (**2006**) *Biotechnol. Lett*. 26: 331 –336.
[22] Pagnanelli, F., Papini, M. P., Toro, L., Trifoni, M., and F. Veglio(**2000**). *Environ. Sci. Technol.* 34 (13), 2773–2778.
[23] Morrison R.T. and Boyd R.N.(**2002**):Organic chemistry, sixth Ed. Pearson Education Ltd, Singapore. PP 1143 – 1204.
[24] Yee, N., Benning, L. G., Phoenix, V. R., and Ferris, F. G.(**2004**). *Environ. Sci. Technol*. 38:775–782.
[25] Jnr, M. H., and Spiff, A. I.(**2004**). *Eur. J. Biotechnol*. 7 (**2004**) 313–323.
[26] Bhatti, N. H., Hanif, M. A., Nadeema, R., Ahmada, N. R., and Ansari, T. M.(**2006**). *J. Hazard Mater*. 139: 345-355.
[27] Saradhi B. V, Rao S. R. K, Kumar Y. P, Vijetha P, Rao K. V and Kalyami G(**2010**). *International Journal of Chemical Engineering Research*. Vol.2(2).Pp 139 – 148.
[28] Lokeshwari, N., and Keshava, Joshi(**2009**). *Global J. Environ. Res.*, 3 (1): 29-35.
[29] Pattabhi, S., Madhavakrishan S., Manickavasagam, K., Rasppan K., Venekatesh R., and Shabudeen, P. S. S (**2008**). *E. Journal of Chemistry.*, 5(4).Pp 761 – 769.
[30] Gonzalez, F., Romera, E., Ballester, A., Blazquez, M. L., and Munoz, J. A(**2006**). *J. Crit. Rev. Biotechnol*. 26: 223 - 235
[31] Lagergren S (**1898**). *Hand linger*.24(4):1-39.
[32] Ho, Y. S., and McKay, G.(**1999**). *Water Res*. 33: 578–584.
[33] McKay, G., and Ho, Y. S.(**1999**) *Process Biochem*. 34: 451–465.
[34] Mahamadi, C and Torto, N. (**2007**). *EJEAFChe*, 6(4): 2165 – 2172.
[35] Dursun, A. Y.(**2006**). *Biochem. Eng. J*. 28: 187 – 195.
[36] Raghavarao, J., Sivaprakash, A., Unninair, B. and Aravindhan, R. (**2009**). *Applied Ecology and Environmental Research*, 7(1): 45-57.
[37] Holan, Z. R., and Volesky, B.(**1994**). *Biotechnol. Bioeng*. 43:1001–1009.